23

Asymptotic Expansion Homogenisation and Multiscale Topology Optimisation of Composite Structures

João A. Oliveira, Joaquim Pinho-da-Cruz and Filipe Teixeira-Dias
Departamento de Engenharia Mecânica, Universidade de Aveiro
Portugal

1. Introduction

Composite materials are among the most prominent materials today, both in terms of applications and development. Nevertheless, their complex structure and heterogeneous nature lead to difficulties, both in the prediction of its properties and on the achievement of the ideal constituent distributions. Homogenisation procedures may provide answers in both cases. With this in mind, the main focus of this chapter is to show the importance of computational procedures for this task, mainly in terms of the different applications of Asymptotic Expansion Homogenisation (AEH) to heterogeneous periodic media and, above all, composite materials. First of all, it is noteworthy that the detailed numerical modelling of the mechanical behaviour of composite material structures tends to involve high computational costs. In this scope, the use of homogenisation methodologies can lead to significant benefits. These techniques allow the simplification of a heterogeneous medium using an equivalent homogenous medium and macrostructural behaviour laws obtained from microstructural information. Furthermore, composite materials typically have heterogeneities with characteristic dimensions significantly smaller than the dimensions of the structural component itself. If the distribution of the heterogeneities is roughly periodic, it can usually be approximated by a detailed periodic representative unit-cell. Thus, the Asymptotic Expansion Homogenisation (AEH) method is an excellent methodology to model physical phenomena on media with periodic microstructure, as well as a useful technique to study the mechanical behaviour of structural components built with composite materials. In terms of computational implementation, the main advantages of this method are (i) the fact that it allows a significant reduction of the number of degrees of freedom and (ii) the capability to find the stress and strain microstructural fields associated with a given macrostructural equilibrium state. In fact, unlike other common homogenisation methods, the AEH leads to explicit mathematical equations to characterise those fields, that is, to perform a localisation.

On the other hand, topology optimisation typically deals with material distributions to achieve the best behaviour for a given objective. The common approach to structural topology optimisation uses a variety of compliance minimisation (stiffness maximisation) procedures and functions. When analysing composite materials, these strategies often lead to multiscale procedures, either as a way to relax the initial discrete problem or in an effort to attain both optimal global structure and optimal microstructure. In this sense, the integration of AEH

procedures in topology optimisation appears in different ways, either through simultaneous multiscale optimisation, or taking the influence of one of the scales and optimising the other. In this sense, this chapter shows the four main approaches to the integration of AEH in topology optimisation procedures: structure optimisation for a given composite microstructure; microstructure optimisation for a given structure; simultaneous optimisation of both scales (hierarchical approach); and material design. The problems are solved on a multiload multiobjective thermoelastic in-house developed computational platform.
The authors thus show the use of AEH procedures and equations both to evaluate homogenised composite materials and to find the ideal material distribution for a given problem. This chapter aims to provide a review of some of the main aspects of these methods and to present some illustrative examples.

2. Asymptotic Expansion Homogenisation

The Asymptotic Expansion Homogenisation (AEH) method is used to solve problems that involve physical phenomena on continuous media with periodic microstructures. It is a useful technique to study the behaviour of structural components built from composite materials, with some advantages over other methods. On one hand, it allows a significant reduction of the problem size and, on the other hand, it has the capability to characterise surface conduction heat flux, strain and stress microfields. AEH leads to specific equations that characterise these fields in a process called localisation, not found on most homogenisation methods. The localisation process is essentially the inverse of the homogenisation process.

2.1 Differential formulation of thermal and thermoelastic problems

A linear thermoelastic heterogeneous material fills a solid[1] $\Omega \in \mathbb{R}^3$ and has a microstructure defined by the periodic distribution of a Representative Unit-Cell (RUC) in the space Y (see Fig. 1). As periodic microstructure materials usually have a small relation $\varepsilon \ll 1$ between the characteristic dimensions of both domains, the thermomechanical response of these materials has periodic oscilations of the resulting temperature, displacement, conduction heat flux, stress and strain fields. These oscillations rise from the periodic heterogeneities and are seen in a neighbourhood ε of any point in Ω. It is thus natural to assume the existence of two separate scales $\mathbf{x}$ and $\mathbf{y}$ where the behaviour of the material on the macroscale and microscale, respectively, takes place. The variables associated to different fields are then functionally dependent of both systems $\mathbf{x}$ and $\mathbf{y}$, where

$$\mathbf{y} = \mathbf{x}/\varepsilon. \tag{1}$$

This functional dependence in $\mathbf{y}$ is periodic in the domain Y, a property usually referred to as Y-periodicity.
In terms of thermoelastic properties, Y-periodicity of the microstructural heterogeneity gives Y-periodic thermal conductivity $\mathbf{k}$, thermal expansion $\boldsymbol{\alpha}$ and elasticity $\mathbf{D}$ tensors. On the other hand, macroscale material homogeneity results in a non-direct dependency between these tensors and the macroscale coordinate system $\mathbf{x}$. In this context, these constitutive tensors are

[1] The open set $\Omega \in \mathbb{R}^3$ is limited by the boundary Γ.

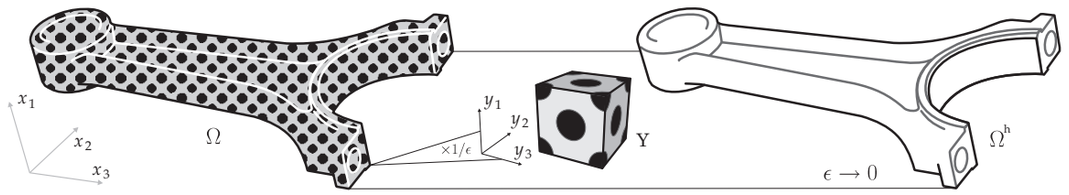

Fig. 1. Heterogeneous thermoelastic material Ω and representative unit-cell Y used in the microscale problem of the asymptotic expansion homogenisation, resulting, with $\varepsilon \to 0$, on the homogeneous material Ω^{h}.

defined as

$$k_{ij} = k_{ij}(\mathbf{y}), \tag{2}$$

$$\alpha_{ij} = \alpha_{ij}(\mathbf{y}) \quad \text{and} \tag{3}$$

$$D_{ijkl} = D_{ijkl}(\mathbf{y}), \tag{4}$$

respectively. On the macroscale coordinate system, $\mathbf{x}$, microstructural heterogeneities manifest over a period ε^{-1} times smaller than the characteristic dimensions of the space Y. Then, according to equation 1,

$$k^{\varepsilon}_{ij}(\mathbf{x}) = k_{ij}(\mathbf{x}/\varepsilon), \tag{5}$$

$$\alpha^{\varepsilon}_{ij}(\mathbf{x}) = \alpha_{ij}(\mathbf{x}/\varepsilon) \quad \text{and} \tag{6}$$

$$D^{\varepsilon}_{ijkl}(\mathbf{x}) = D_{ijkl}(\mathbf{x}/\varepsilon), \tag{7}$$

where the index ε states that $\mathbf{k}$, $\boldsymbol{\alpha}$ and $\mathbf{D}$ are εY-periodic in $\mathbf{x}$. In this sense, the thermal steady-state problem is described by the equilibrium equation and the Fourier's law for heat conduction (Cioranescu & Donato, 1999)

$$\frac{\partial q^{\varepsilon}_i}{\partial x^{\varepsilon}_i} - Q = 0 \quad \text{in} \quad \Omega \quad \text{and} \tag{8}$$

$$q^{\varepsilon}_i = -k^{\varepsilon}_{ij}\frac{\partial T^{\varepsilon}}{\partial x^{\varepsilon}_j} \quad \text{in} \quad \Omega, \tag{9}$$

for $i, j = 1, \ldots, 3$. q_i are the components of the surface conduction heat fluxes. Q it the rate of heat generation per unit volume and T the temperature field. The boundary of Ω is defined by the surfaces $\Gamma_{\mathrm{D_T}}$, $\Gamma_{\mathrm{N_T}}$ and $\Gamma_{\mathrm{R_T}}$. These are related to the Dirichlet, Neumann and Robin boundary conditions [2]

$$T^{\varepsilon} = \bar{T} \quad \text{in} \quad \Gamma_{\mathrm{D_T}}, \tag{10}$$

$$q^{\varepsilon}_i n_i = -\bar{q} \quad \text{in} \quad \Gamma_{\mathrm{N_T}} \quad \text{and} \tag{11}$$

$$q^{\varepsilon}_i n_i = h_{\mathrm{c}}(T^{\varepsilon} - T_{\infty}) \quad \text{in} \quad \Gamma_{\mathrm{R_T}}, \tag{12}$$

where $\Gamma_{\mathrm{D_T}} \cup \Gamma_{\mathrm{N_T}} \cup \Gamma_{\mathrm{R_T}} = \Gamma$ and $\Gamma_{\mathrm{D_T}} \cap \Gamma_{\mathrm{N_T}} = \Gamma_{\mathrm{D_T}} \cap \Gamma_{\mathrm{R_T}} = \Gamma_{\mathrm{N_T}} \cap \Gamma_{\mathrm{R_T}} = \varnothing$. $\bar{T}$ and $\bar{q}$ are prescribed temperature and surface conduction heat flux values, respectively. n_i are the components of an outward unit vector, orthogonal to the surfaces $\Gamma_{\mathrm{N_T}}$ or $\Gamma_{\mathrm{R_T}}$. h_{c} and T_{∞}

[2] Radiation processes are note considered in this work.

are the convection coefficient and ambient temperature, respectively. The temperature field is the solution to the thermal problem is the solution $T^\varepsilon \in \mathrm{V}_\Omega^0$ of the variational problem

$$\int_\Omega k_{ij}^\varepsilon \frac{\partial T^\varepsilon}{\partial x_j^\varepsilon}\frac{\partial v}{\partial x_i^\varepsilon}\mathrm{d}\Omega = \int_\Omega Qv\mathrm{d}\Omega + \int_{\Gamma_{\mathrm{N_T}}} \bar{q}v\mathrm{d}\Gamma - \int_{\Gamma_{\mathrm{R_T}}} h_\mathrm{c}\left(T^\varepsilon - T_\infty\right)v\mathrm{d}\Gamma, \quad \forall v \in \mathrm{V}_\Omega^0, \tag{13}$$

where V_Ω^0 is the set of continuous functions, sufficiently regular and zero-valued in $\Gamma_{\mathrm{D_T}}$.
The heterogeneous material is made of $n > 1$ homogeneous materials, making the thermal problem a set of n problems with equations equivalent to expression 8, having temperature and surface flux continuity conditions on every interface between subdomains (Lewis et al., 1996).
Assuming infinitesimal strains associated to a quasi-static process, the linear thermoelasticity problem is described by the following equilibrium equations, strain-displacement relations and constitutive relations (Duhamel-Neumann law) (Cioranescu & Donato, 1999)

$$\frac{\partial \sigma_{ij}^\varepsilon}{\partial x_j^\varepsilon} + b_i = 0 \quad \text{in} \quad \Omega, \tag{14}$$

$$\epsilon_{ij}^\varepsilon = \frac{1}{2}\left(\frac{\partial u_i^\varepsilon}{\partial x_j^\varepsilon} + \frac{\partial u_j^\varepsilon}{\partial x_i^\varepsilon}\right) \quad \text{in} \quad \Omega \quad \text{and} \tag{15}$$

$$\sigma_{ij}^\varepsilon = D_{ijkl}^\varepsilon \epsilon_{kl}^\varepsilon - \Delta T^\varepsilon \beta_{ij}^\varepsilon \quad \text{in} \quad \Omega, \tag{16}$$

respectively, where

$$\Delta T^\varepsilon = T^\varepsilon - T_0 \quad \text{and} \tag{17}$$

$$\beta_{ij}^\varepsilon = D_{ijkl}^\varepsilon \alpha_{kl}^\varepsilon = \beta_{ij}^\varepsilon(\mathbf{x}/\varepsilon). \tag{18}$$

σ_{ij} and ϵ_{ij} the components of the Cauchy stress tensor and strain tensor, respectively. b_i and u_i represent the components of the volume loads and displacements, respectively. T_0 is the reference temperature and β_{ij} are the components of the thermal moduli tensor. If $\Delta T^\varepsilon = 0$ or $\beta_{ij}^\varepsilon = 0$, the problem becomes the purely mechanical linear elastic problem. The boundary of Ω is defined by the surfaces $\Gamma_{\mathrm{D_u}}$ and $\Gamma_{\mathrm{N_u}}$. These are associated to Dirichlet and Neumann boundary conditions

$$u_i^\varepsilon = \bar{u}_i \quad \text{in} \quad \Gamma_{\mathrm{D_u}} \quad \text{and} \tag{19}$$

$$\sigma_{ij}^\varepsilon n_j = \bar{t}_i \quad \text{in} \quad \Gamma_{\mathrm{N_u}}, \tag{20}$$

respectively, where $\Gamma_{\mathrm{D_u}} \cup \Gamma_{\mathrm{N_u}} = \Gamma$ and $\Gamma_{\mathrm{D_u}} \cap \Gamma_{\mathrm{N_u}} = \varnothing$. $\bar{u}_i$ and $\bar{t}_i$ are prescribed displacement and surface load values, respectively. n_j are components of an outward unit vector, orthogonal to surface $\Gamma_{\mathrm{N_u}}$.
Solving the thermoelastic problem consists of determining the displacement field that is the solution $\mathbf{u}^\varepsilon \in \mathrm{V}_\Omega^0$ of the variational problem

$$\int_\Omega D_{ijkl}^\varepsilon \frac{\partial u_k^\varepsilon}{\partial x_l^\varepsilon}\frac{\partial v_i}{\partial x_j^\varepsilon}\mathrm{d}\Omega = \int_\Omega \left(T^\varepsilon - T_0\right)\beta_{ij}^\varepsilon \frac{\partial v_i}{\partial x_j^\varepsilon}\mathrm{d}\Omega + \int_\Omega b_i v_i \mathrm{d}\Omega + \int_{\Gamma_{\mathrm{N_u}}} \bar{t}_i v_i \mathrm{d}\Gamma, \quad \forall \mathbf{v} \in \mathrm{V}_\Omega^0, \tag{21}$$

where V_Ω^0 is the set of funcions, continuous, sufficiently regular and zero-valued in $\Gamma_{\mathrm{D_u}}$.
The heterogeneous material is made of $n > 1$ homogeneous materials, from which the linear thermoelasticity problem consists of n equations similar to equation 14, associated to displacement and surface load continuity conditions on the interfaces of the different material subdomains.

2.2 Homogenised thermal and thermoelastic problems

With the existence of two different scales, associated to behaviour levels over the macroscale Ω and microscale Y, the temperature and displacement fields are approximated using the respective asymptotic expansions in ε:

$$T^{\varepsilon}(\mathbf{x}) = T^{(0)}(\mathbf{x},\mathbf{y}) + \varepsilon T^{(1)}(\mathbf{x},\mathbf{y}) + \varepsilon^2 T^{(2)}(\mathbf{x},\mathbf{y}) + \cdots \quad \text{and} \tag{22}$$

$$u_i^{\varepsilon}(\mathbf{x}) = u_i^{(0)}(\mathbf{x},\mathbf{y}) + \varepsilon u_i^{(1)}(\mathbf{x},\mathbf{y}) + \varepsilon^2 u_i^{(2)}(\mathbf{x},\mathbf{y}) + \cdots, \tag{23}$$

where $T^{(r)}(\mathbf{x},\mathbf{y})$ and $u_i^{(r)}(\mathbf{x},\mathbf{y})$, with $r \in \mathbb{N}_0$, are Y-periodic functions in $\mathbf{y}$, classified as the r^{th} order temperature field correctors and displacement field correctors, respectively. According to equation 1, using the chain rule of function derivatives,

$$\frac{\partial \cdot}{\partial x_i^{\varepsilon}} = \frac{\partial \cdot}{\partial x_i} + \frac{1}{\varepsilon}\frac{\partial \cdot}{\partial y_i}. \tag{24}$$

In this context, including the temperature asymptotic expansion (Eq. 22) in the Fourier's equations for heat conduction (Eq. 9) and on the Duhamel-Neumann law (Eq. 16), and including the displacement asymptotic expansion (Eq. 23) in the linearised strain-displacement relations (Eq. 15), result in the linearised thermoelastic problem. The temperature field $T^{(0)}$ is the solution of the homogenised thermal problem

$$\frac{\partial \Xi_i}{\partial x_i} - Q = 0 \quad \text{in} \quad \Omega, \tag{25}$$

$$T^{(0)} = \bar{T} \quad \text{in} \quad \Gamma_{\mathrm{D_T}}, \tag{26}$$

$$\Xi_i n_i = -\bar{q} \quad \text{in} \quad \Gamma_{\mathrm{N_T}}, \tag{27}$$

$$\Xi_i n_i = h_{\mathrm{c}}\left(T^{(0)} - T_{\infty}\right) \quad \text{in} \quad \Gamma_{\mathrm{R_T}}, \quad \text{with} \tag{28}$$

$$\Xi_i = -k_{ij}^{\mathrm{h}}\frac{\partial T^{(0)}}{\partial x_j} \quad \text{in} \quad \Omega, \tag{29}$$

where Ξ_i are the components of the macrostructural homogenised superficial conduction heat fields and k_{ij}^{h} are the components of the homogenised thermal conductivity tensor, defined as

$$k_{ik}^{\mathrm{h}} = \frac{1}{|\mathrm{Y}|}\int_{\mathrm{Y}} k_{ij}(\mathbf{y})\left(\mathrm{I}_j^k - \frac{\partial \mathrm{Y}^k}{\partial y_j}\right)\mathrm{d}Y. \tag{30}$$

$\mathrm{I}_j^k = \delta_{jk}$ is the Kronecker delta and Y^k are the components of the thermal characteristic displacement field tensor (Pinho-da-Cruz, 2007). These are the solutions $\mathrm{Y}^k \in \widetilde{\mathrm{V}}_{\mathrm{Y}}$ of the auxiliary microstructural variational problem

$$\int_{\mathrm{Y}} k_{ij}\frac{\partial \mathrm{Y}^k}{\partial y_j}\frac{\partial v}{\partial y_i}\mathrm{d}Y = \int_{\mathrm{Y}} k_{ik}\frac{\partial v}{\partial y_i}\mathrm{d}Y, \quad \forall v \in \widetilde{\mathrm{V}}_{\mathrm{Y}}, \tag{31}$$

where $\widetilde{\mathrm{V}}_{\mathrm{Y}}$ is the set of Y-periodic continuous functions, sufficiently regular and with an average value[3] equal to zero in Y. The existence of average values equal to zero in Y for the

[3] The average value on a function $\Phi(\mathbf{x},\mathbf{y})$, Y-periodic in Y, is defined by $< \Phi >_{\mathrm{Y}} = \frac{1}{|\mathrm{Y}|}\int_{\mathrm{Y}} \Phi(\mathbf{x},\mathbf{y})\,\mathrm{d}Y$.

solutions of the equations 31 is an unicity condition for the thermal characteristic displacement field tensor $\mathbf{Y}$ (Sanchez-Hubert & Sanchez-Palencia, 1992).
Concerning the displacement field $u_i^{(0)}$, it is the solution of the homogenised thermoelasticity problem

$$\frac{\partial \Sigma_{ij}}{\partial x_j} + b_i = 0 \quad \text{in} \quad \Omega, \tag{32}$$

$$u_i^{(0)} = \bar{u}_i \quad \text{in} \quad \Gamma_{\mathrm{D_u}}, \tag{33}$$

$$\Sigma_{ij} n_j = \bar{t}_i \quad \text{in} \quad \Gamma_{\mathrm{N_u}}, \quad \text{with} \tag{34}$$

$$\Sigma_{ij} = D^{\mathrm{h}}_{ijkl} \frac{\partial u_k^{(0)}}{\partial x_l} - \left(T^{(0)} - T_0 \right) \beta^{\mathrm{h}}_{ij} \quad \text{in} \quad \Omega, \tag{35}$$

where Σ_{ij} are components of the macrostructural homogenised stress tensor. D^{h}_{ijkl} and β^{h}_{ij} are the components of the homogenised elasticity and thermal moduli tensors, respectively, defined as

$$D^{\mathrm{h}}_{ijmn} = \frac{1}{|\mathrm{Y}|} \int_{\mathrm{Y}} D_{ijkl}\left(\mathbf{y}\right) \left(\mathrm{I}^{mn}_{kl} - \frac{\partial \chi_k^{mn}}{\partial y_l} \right) \mathrm{d}Y \quad \text{and} \tag{36}$$

$$\beta^{\mathrm{h}}_{ij} = \frac{1}{|\mathrm{Y}|} \int_{\mathrm{Y}} \left[\beta_{ij}\left(\mathbf{y}\right) - D_{ijkl}\left(\mathbf{y}\right) \frac{\partial \Psi_k}{\partial y_l} \right] \mathrm{d}Y \,. \tag{37}$$

$\mathrm{I}^{mn}_{kl} = \delta_{km}\delta_{ln}$, where δ_{ij} is the symbol for the Kronecker delta. χ_k^{mn} and Ψ_k are the components of the mechanical characteristic displacement field tensor and thermomechanical characteristic displacement field tensor, respectively (Pinho-da-Cruz, 2007). These fields are the solutions $\chi_k^{mn} \in \widetilde{\mathrm{V}}_{\mathrm{Y}}$ and $\Psi_k \in \widetilde{\mathrm{V}}_{\mathrm{Y}}$ of the microstructural variational auxiliary problems

$$\int_{\mathrm{Y}} D_{ijkl} \frac{\partial \chi_k^{mn}}{\partial y_l} \frac{\partial v_i}{\partial y_j} \mathrm{d}Y = \int_{\mathrm{Y}} D_{ijmn} \frac{\partial v_i}{\partial y_j} \mathrm{d}Y, \quad \forall v_i \in \widetilde{\mathrm{V}}_{\mathrm{Y}}, \quad \text{and} \tag{38}$$

$$\int_{\mathrm{Y}} D_{ijkl} \frac{\partial \Psi_k}{\partial y_l} \frac{\partial v_i}{\partial y_j} \mathrm{d}Y = \int_{\mathrm{Y}} \beta_{ij} \frac{\partial v_i}{\partial y_j} \mathrm{d}Y, \quad \forall v_i \in \widetilde{\mathrm{V}}_{\mathrm{Y}}, \tag{39}$$

where $\widetilde{\mathrm{V}}_{\mathrm{Y}}$ is the set of Y-periodic functions, continuous and sufficiently regular, with an average value equal to zero in Y. Once again, the existence of average values equal to zero in Y for the solutions of the equations 38 and 39 is an unicity condition for the tensor $\boldsymbol{\chi}$ of the mechanical characteristic displacement field (Sanchez-Hubert & Sanchez-Palencia, 1992) and for the tensor $\boldsymbol{\Psi}$ of the thermomechanical characteristic displacement field, respectively.
Note that the usage of two scales in this application is based on the assumption of the existence of periodic oscillations os the resulting temperature and displacement fields that result from the periodicity of the microstructural heterogeneous detail. These oscillations should superimpose the macroscopic fields, where the heterogeneous details are not directly considered. Is this sense, for first-order approximations of the temperature and displacement fields, these oscillations can be seen as fluctuations around a macroscopic average value, as illustrated in figure 2.

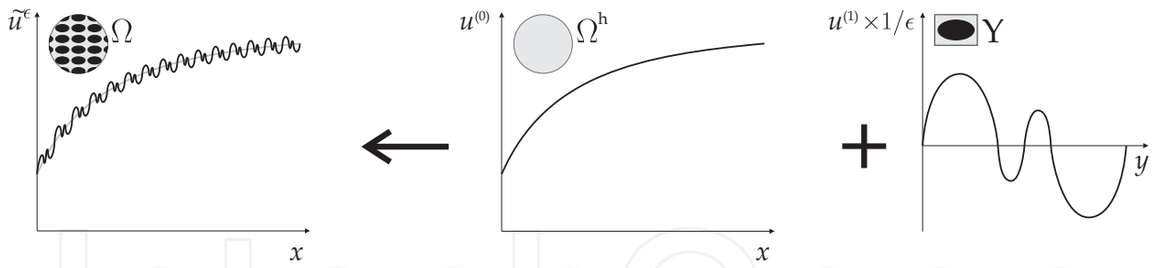

Fig. 2. Illustration of the asymptotic expansion homogenisation first-order approximation for the displacement field for a one-dimensional case. The displacement field in Ω is approximated adding the Y−periodic microscale first-order fluctuations to the homogenised macroscale Ω^{h} field.

2.3 Conventional methodologies

2.3.1 Conventional homogenisation

In practice, a significant part of structural applications based on periodic microstructure materials has a scale factor $\varepsilon \ll 1$. In this sense, first-order approximations for the temperature and displacement fields are adequate representations (see Eqs. 22 and 23). This simplifies the asymptotic expansion methodology, resulting in the conventional homogenisation methodology (Terada, 1996). This is a rigorous mathematical technique, in which the initial problems are approximated by a two-scale procedure. In this, the global problem becomes a conventional structural problem with a homogeneous material, using constitutive information taken from the solutions of the microscale problems. These, on the other hand, allow the study of the microstructural detail using a representative unit-cell. The homogenised properties are calculated from the solutions of the microscale problems with periodicity constraints (see Eqs. 31 and 30, 38 and 36, and 39 and 37).

In this sense, the numerical gains of this method are considerable, since the number of degrees of freedom associated to a detailed discretisation is significantly reduced. The microstructural details are instead defined on a single representative unit-cell, while the macrostructure is modelled as is it was a homogeneous medium.

2.3.2 Conventional localisation

Another advantage of the asymptotic expansion homogenisation is that it allows the characterisation of the microstructural surface conduction heat flux, strain and stress fields. In fact, contrary to the other usual homogenisation methods, this method provides mathematical expressions that define the microstructural levels of these fields. This process, opposite to the homogenisation, is called localisation (see Fig. 3).

Considering first-order approximations, the microstructural surface conduction heat flux field defined on the conventional localisation methodology is (Pinho-da-Cruz, 2007)

$$q_i^{(1)}(\mathbf{x},\mathbf{y}) = k_{ij}(\mathbf{y}) \left(\frac{\partial \mathrm{Y}^k}{\partial y_j} - \mathrm{I}_j^k \right) \frac{\partial T^{(0)}}{\partial x_k} . \tag{40}$$

The localised microstructural strain field, on the other hand, is defined as

$$\epsilon_{ij}^{(1)}(\mathbf{x},\mathbf{y}) = \Im_{ij}^{kl} \left[\left(\mathrm{I}_{kl}^{mn} - \frac{\partial \chi_k^{mn}}{\partial y_l} \right) \frac{\partial u_m^{(0)}}{\partial x_n} + \frac{\partial \Psi_k}{\partial y_l} \left(T^{(0)} - T_0 \right) \right] , \tag{41}$$

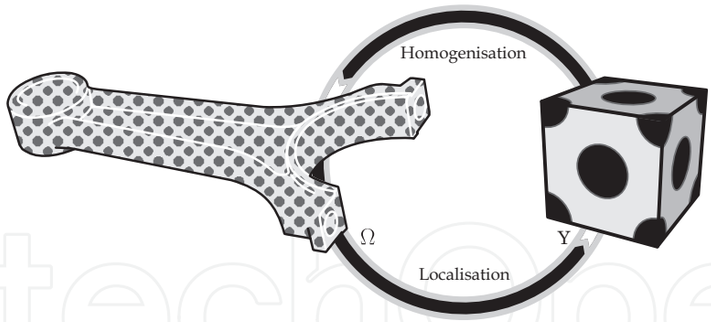

Fig. 3. Data flux between the macroscale Ω and microscale Y with the homogenisation and localisation procedures.

where

$$\Im_{ij}^{kl} = \frac{1}{2}\left(\delta_{ik}\delta_{jl} + \delta_{il}\delta_{jk}\right). \tag{42}$$

In turn, the localised stress field is defined as

$$\sigma_{ij}^{(1)}(\mathbf{x},\mathbf{y}) = D_{ijkl}(\mathbf{y})\left(\mathrm{I}_{kl}^{mn} - \frac{\partial \chi_k^{mn}}{\partial y_l}\right)\frac{\partial u_m^{(0)}}{\partial x_n} + \left[D_{ijkl}(\mathbf{y})\,\frac{\partial \Psi_k}{\partial y_l} - \beta_{ij}(\mathbf{y})\right]\left(T^{(0)} - T_0\right). \tag{43}$$

Equations 40, 41 and 43 allow, for a given point $\mathbf{x}$, the definition of the approximate values for the respective fields within the microstructural heterogeneities. On the other hand, the homogenised macrostructural heat flux, Ξ_i, and stress, Σ_{ij}, fields, being by definition the average of the microstructural heat flux $q_i^{(1)}$ and stress $\sigma_{ij}^{(1)}$ fields in Y, are unable to represent any microstructural fluctuations and lack detail.
For further details on the mathematical and numerical basis of the asymptotic expansion homogenisation method and its applications, please consult the references (Guedes & Kikuchi, 1990; Oliveira et al., 2009; Pinho-da-Cruz, 2007; Pinho-da-Cruz et al., 2008; 2009).

3. AEH and topology optimisation

In the context of topology optimisation aplications, the effective number of different homogeneous materials on the microstructure of a given heteregeneous material depends on the density distribution that results from the use of the SIMP (Solid Isotropic Material with Penalisation) method on the microscale. The homogenised constitutive tensors, $\mathbf{D}^{\mathrm{h}}$, $\boldsymbol{\beta}^{\mathrm{h}}$ and $\mathbf{k}^{\mathrm{h}}$ can be calculated using the AEH (see Eqs. 36, 37 and 30). However, their use in the topology optimisation procedures presented on the second part of this chapter requires a small change to the definition of the local properties within the microscale. Instead of having different base materials, the material in each point $\mathbf{y}$ is defined by the SIMP power-law method, thus affecting a single base material with different density values μ (Bendsøe & Sigmund, 2003), *i.e.*

$$\mathbf{D}_{e_y} = \mathbf{D}(\mu) = \mu^p \mathbf{D}^0, \tag{44}$$

$$\boldsymbol{\beta}_{e_y} = \boldsymbol{\beta}(\mu) = \mathbf{D}(\mu)\boldsymbol{\alpha}(\mu) = \mu^p \mathbf{D}^0 \mu^p \boldsymbol{\alpha}^0 = \mu^{2p}\boldsymbol{\beta}^0 \quad \text{and} \tag{45}$$

$$\mathbf{k}_{e_y} = \mathbf{k}(\mu) = \mu^p \mathbf{k}^0, \tag{46}$$

where the density $\mu = \mu(\mathbf{y})$ may vary continuously within[4] $0 \leq \mu \leq 1$ and p is an intermediate density penalisation factor, aimed at obtaining discrete results for the optimisation problem, with two well defined material phases. From this, equations 36, 37 and 30 are, respectively, slightly changed to

$$D^{\mathrm{h}}_{ijmn} = \frac{1}{|\mathrm{Y}|}\int_{\mathrm{Y}} D_{ijkl}(\mu)\left(\mathrm{I}^{mn}_{kl} - \frac{\partial \chi^{mn}_{k}}{\partial y_l}\right)\mathrm{d}Y\,, \tag{47}$$

$$\beta^{\mathrm{h}}_{ij} = \frac{1}{|\mathrm{Y}|}\int_{\mathrm{Y}} \left(\beta_{ij}(\mu) - D_{ijkl}(\mu)\frac{\partial \Psi_k}{\partial y_l}\right)\mathrm{d}Y \quad \text{and} \tag{48}$$

$$k^{\mathrm{h}}_{ik} = \frac{1}{|\mathrm{Y}|}\int_{\mathrm{Y}} k_{ij}(\mu)\left(\mathrm{I}^{k}_{j} - \frac{\partial \mathrm{Y}^{k}}{\partial y_j}\right)\mathrm{d}Y\,. \tag{49}$$

Equations 47 and 49 may as well be written in variational form (Bendsøe, 1995) as

$$D^{\mathrm{h}}_{ijmn} = \frac{1}{|\mathrm{Y}|}\int_{\mathrm{Y}} D_{pqkl}(\mu)\left(\mathrm{I}^{ij}_{pq} - \frac{\partial \chi^{ij}_{p}}{\partial y_q}\right)\left(\mathrm{I}^{mn}_{kl} - \frac{\partial \chi^{mn}_{k}}{\partial y_l}\right)\mathrm{d}Y \quad \text{and} \tag{50}$$

$$k^{\mathrm{h}}_{ik} = \frac{1}{|\mathrm{Y}|}\int_{\mathrm{Y}} k_{lj}(\mu)\left(\mathrm{I}^{i}_{l} - \frac{\partial \mathrm{Y}^{i}}{\partial y_l}\right)\left(\mathrm{I}^{k}_{j} - \frac{\partial \mathrm{Y}^{k}}{\partial y_j}\right)\mathrm{d}Y\,, \tag{51}$$

respectively.
Another aspect of the possible material distribution affects the desired bounds in terms of properties within the microscale. The presented SIMP format is usually applied for material interpolation between material and void. However, when working with composite materials, the bounds will be determined by two different constituent materials. One of the most straightforward ways to fulfil this requirement is slightly changing the power-law (Bendsøe & Sigmund, 1999; Sigmund, 2007). On one hand, the general material property P becomes

$$P(\mu) = \mu^p P_1 + (1-\mu^p)P_2 \tag{52}$$

where $P_1 > P_2$. This material interpolation scheme allows property P to vary between the bounds of material 1 and material 2. Furthermore, if $P_2 = P_{\min}$, it results in an interpolation between material and void. In either case, as used in this work, this power-law can be redefined as

$$P(\mu) = \mu^p P_1 + (1-\mu^p)d_m P_1 = \left[\mu^p + d_m(1-\mu^p)\right]P_1\,, \tag{53}$$

where $d_m = P_{\min}/P_1$. Alternatively, the modified SIMP (Bendsøe & Sigmund, 1999; Sigmund, 2007)

$$P(\mu) = P_{\min} + \mu^p(P_1 - P_{\min}) \tag{54}$$

has the same practical implications. Both in equations 53 and 54, $P_{\min}$ is the minimum value for the property P, different from zero to avoid singularities and numerical conditioning problems. Furthermore, these alternatives have some advantages over the original SIMP, most of all the fact that the minimum for P is now independent of the penalty exponent. They allow the use of multiphase materials, instead of the original cellular materials, and are more flexible for a wider variety of filtering techniques (Sigmund, 2007).

[4] In practice, it is usual to use a minimum value for the density $\mu \geq \mu_{\min} > 0$, in order to avoid numerical problems if $\mu = 0$.

4. Multiscale topology optimisation

Topology optimisation in structural mechanics consists of searching for the optimal material distribution within a certain admissible domain. This distribution, dependent on density variables, varies between high and low density regions. As a matter of fact, the initial definition of the problem is discrete, in which the variable can only take the values 1 (dense material) or 0 (void or soft phase). Among several others, one of the strategies for relaxing this problem is allowing the existence of intermediate densities and giving it physical meaning by association with coherent microstructures of cellular or composite material. This approach leads to multiscale procedures and is usually classified of homogenisation method, leading to several different implementations and using several methods to deal with the local problem (Allaire, 2001; Bendsøe & Kikuchi, 1988; Bendsøe & Sigmund, 2003; Diaz & Lipton, 1997; Guedes et al., 2006; Hassani & Hinton, 1999; Rodrigues et al., 2002; Theocaris & Stavroulakis, 1998; 1999).
In this sense, the authors show a multilevel or hierarchical methodology, for both thermoelasticity and heat conduction. A detailed description of the hierarchical methodologies applied to elasticity can be consulted in the references (Coelho et al., 2008; Rodrigues et al., 2002; Theocaris & Stavroulakis, 1998; 1999). The Asymptotic Expansion Homogenisation method is used in the local problem of this application, both in terms of constitutive analysis and sensitivity evaluation.

4.1 Hierarchical thermoelastic problem

Structural topology optimisation typically searches for the material distribution that minimize compliance (maximises stiffness). In its usual form, this is evaluated using the strain energy function as a measure of compliance or flexibility of the structure, defined as

$$S = \frac{1}{2}\int_{\Omega} \rho^{p}\boldsymbol{\varepsilon}(\mathbf{u}) : \mathbf{D}^{0} : \boldsymbol{\varepsilon}(\mathbf{u})\mathrm{d}\Omega \tag{55}$$

where $\rho = \rho(\mathbf{x})$ is the macrostructural density value, or using the work of exterior loads (*compliance*)

$$W = \int_{\Omega} \mathbf{b}\cdot\mathbf{u}\mathrm{d}\Omega + \int_{\Gamma_{\mathrm{N_u}}} \bar{\mathbf{t}}\cdot\mathbf{u}\mathrm{d}\Gamma\,. \tag{56}$$

$\mathbf{b}$ and $\bar{\mathbf{t}}$ are the volume and surface loads, respectively. These two functions can be used to define the total potential energy

$$P = S - W = \frac{1}{2}\int_{\Omega} \rho^{p}\boldsymbol{\varepsilon}(\mathbf{u}) : \mathbf{D}^{0} : \boldsymbol{\varepsilon}(\mathbf{u})\mathrm{d}\Omega - \left(\int_{\Omega} \mathbf{b}\cdot\mathbf{u}\mathrm{d}\Omega + \int_{\Gamma_{\mathrm{N_u}}} \bar{\mathbf{t}}\cdot\mathbf{u}\mathrm{d}\Gamma\right). \tag{57}$$

According to the principle of minimum potential energy, the potential energy is minimised by the displacement field $\mathbf{u}$ that solves the equilibrium problem. This objective function gives an explicit definition of the hierarchical structure of the multiscale problem, which can be written as (Rodrigues et al., 2002; Theocaris & Stavroulakis, 1998; 1999)

$$\max_{\substack{\rho(\mathbf{x}) \\ 0\le\rho(\mathbf{x})\le 1 \\ \int_{\Omega}\rho(\mathbf{x})\mathrm{d}\Omega\le V}} \min_{\substack{\mathbf{u}^{l}\in U \\ l=1,\ldots,L}} \left[\frac{1}{2}\int_{\Omega}\Phi(\rho,\mathbf{u}^{1},\ldots,\mathbf{u}^{L})\mathrm{d}\Omega - \sum_{l=1}^{L} w^{l}\left(\int_{\Omega}\mathbf{b}^{l}\cdot\mathbf{u}^{l}\mathrm{d}\Omega + \int_{\Gamma_{\mathrm{N_u}}}\bar{\mathbf{t}}^{l}\cdot\mathbf{u}^{l}\mathrm{d}\Gamma\right)\right], \tag{58}$$

where $\mathbf{u}$ is the equilibrium displacement field that minimises the potential energy function. This internal minimisation is done solving the equilibrium problem, which can alternatively be seen as an aditional equality constraint. The presented objective function states a multiload configuration with L load cases and corresponding weights w^l. The optimal energy density function $\Phi(\rho, \mathbf{u}^1, \ldots, \mathbf{u}^L)$ is the solution of the local (microscale) problem and is defined as

$$\Phi(\rho, \mathbf{u}^1, \ldots, \mathbf{u}^L) = \max_{\substack{\mu(\mathbf{x},\mathbf{y}) \\ 0 \leq \mu(\mathbf{x},\mathbf{y}) \leq 1 \\ \int_Y \mu(\mathbf{x},\mathbf{y}) \mathrm{d}Y = \rho(\mathbf{x})}} \sum_{l=1}^{L} w^l \left[D^{\mathrm{h}}_{ijkl}(\mu) \varepsilon_{ij}(\mathbf{u}^l) \varepsilon_{kl}(\mathbf{u}^l) \right] . \tag{59}$$

The multiload case was shown on this general definition of the problem but will be dropped for the remaining of this section. It will be recalled whenever necessary. The elastic problem can be extended to include the thermal expansion terms of the thermoelastic problem. In this sense, the strain energy can be updated using the generalised Duhamel-Neumman form of Hooke's law (Fung & Tong, 2005)

$$\sigma_{ij} = D_{ijkl} \varepsilon_{kl} - \beta_{ij} \Delta T \, , \tag{60}$$

rewriting equation 59, for a single-load case, as

$$\Phi(\rho, \mathbf{u}) = \max_{\substack{\mu(\mathbf{x},\mathbf{y}) \\ 0 \leq \mu(\mathbf{x},\mathbf{y}) \leq 1 \\ \int_Y \mu(\mathbf{x},\mathbf{y}) \mathrm{d}Y = \rho(\mathbf{x})}} \left[D^{\mathrm{h}}_{ijkl}(\mu) \varepsilon_{ij}(\mathbf{u}) \varepsilon_{kl}(\mathbf{u}) - 2\beta^{\mathrm{h}}_{ij}(\mu) \varepsilon_{ij}(\mathbf{u}) \Delta T \right] . \tag{61}$$

Note that the local problem results of a localisation process[5] where the local energy density function is maximised according to a macroscale strain tensor. This structure defines two different functionally dependent problems: the global problem, where equilibrium is achieved and the overall objective is evaluated, and a set of microstructural problems, where each of the local response is optimised and constitutive information is obtained. In the local problem, the local density variable $\mu(\mathbf{x}, \mathbf{y})$ is related to the global density variable through the local volume restriction as $\int_Y \mu(\mathbf{x}, \mathbf{y}) \mathrm{d}Y = \rho(\mathbf{x})$.
On a further notice, the global objective function and the overall definition of the hierarchical optimisation problem can also be defined as

$$\min_{\substack{\rho(\mathbf{x}) \\ 0 \leq \rho(\mathbf{x}) \leq 1 \\ \int_\Omega \rho(\mathbf{x}) \mathrm{d}\Omega \leq V \\ \mathbf{Ku} = \mathbf{f}}} \left[\frac{1}{2} \int_\Omega \Phi(\rho, \mathbf{u}) \mathrm{d}\Omega \right] , \tag{62}$$

treated in this case in terms of an equivalent strain energy function and being equivalent, at equilibrium, to the minimisation of the external load work (compliance). Note also that the factor $1/2$ can be simply omitted since it changes the value of the objective but nothing about the optimal solution (Arora, 2004). Furthermore, it is important to state that one of the advantages of the hierarquical structure is that the main procedure is independent of the material modelling. Homogenisation or material modelling may be done over independent modules, born from different methods and not restricted to the AEH used in this work.

[5] Localisation is a generic process where macroscale average values are used to render microstructural detail. The localisation methodology presented for the AEH is specific to that method.

4.2 Optimality conditions

To define the necessary conditions for the optimisation problem, it must be stated in a numerically compatible form. In this sense, according to Rodrigues *et al.* (Rodrigues et al., 2002), the augmented Lagrangian of the outer problem can be written as

$$\mathcal{L} = \min_{u \in U} \left[\frac{1}{2} \int_{\Omega} \Phi(\rho, \mathbf{u}) \mathrm{d}\Omega - \left(\int_{\Omega} \mathbf{b} \cdot \mathbf{u} \mathrm{d}\Omega + \int_{\Gamma_{\mathrm{N_u}}} \bar{\mathbf{t}} \cdot \mathbf{u} \mathrm{d}\Gamma \right) \right. \tag{63}$$
$$\left. - \frac{1}{2c} \left\{ \left[\max \left(0, \Lambda + c \left(\int_{\Omega} \rho \mathrm{d}\Omega - V \right) \right) \right]^2 - \Lambda^2 \right\} \right] ,$$

where c is the penalty parameter and $\Lambda \geq 0$ is the Lagrange multiplier associated to the global volume inequality restriction. Being $\tilde{\mathbf{u}}$ is the displacement field that fulfils global equilibrium, the stationary condition relative to the variable $\rho(\mathbf{x})$ is defined as

$$\frac{1}{2} \frac{\partial \Phi(\rho, \tilde{\mathbf{u}})}{\partial \rho} = \max \left\{ 0, \Lambda + c \left(\int_{\Omega} \rho \mathrm{d}\Omega - V \right) \right\} , \ \forall \mathbf{x} \in \Omega , \text{ with } \rho \in]0, 1[, \tag{64}$$

at point where ρ has intermediate values. At the extremes, this condition becomes an inequality ($\leq$ for $\rho = 0$ and $\geq$ for $\rho = 1$). Note, however, that these extremes are points where there's no need to solve the local problem. The stationary condition relative to the Lagrange multiplier, on the other hand, is

$$\Lambda = \max \left\{ 0, \Lambda + c \left(\int_{\Omega} \rho \mathrm{d}\Omega - V \right) \right\} . \tag{65}$$

Condition 65 implies the fulfilment of the global volume restriction. Condition 64 defines the stability of the Lagrange multiplier Λ at the equilibrium and for the optimal solution, meaning that the derivative of the energy density function at the optimum, relative to the global densities, should be constant at every $\mathbf{x}$ where $0 < \rho < 1$ (Coelho et al., 2008; Rodrigues et al., 2002).

The Lagrangian function for the local problem (Eq. 61) may be written as

$$\mathcal{L} = \left[D^{\mathrm{h}}_{ijkl}(\mu) \varepsilon_{ij}(\tilde{\mathbf{u}}) \varepsilon_{kl}(\tilde{\mathbf{u}}) - 2 \beta^{\mathrm{h}}_{ij}(\mu) \varepsilon_{ij}(\tilde{\mathbf{u}}) \Delta T \right] - \lambda(\tilde{\mathbf{x}}) \left[\int_{Y(\tilde{\mathbf{x}})} \mu \mathrm{d}y - \rho(\tilde{\mathbf{x}}) \right] . \tag{66}$$

This is defined for every $\tilde{\mathbf{x}} \in \Omega$ and the multiplier λ is relative to the local volume restriction, which compares the local density field μ with the global density value for a given point ($\rho(\tilde{\mathbf{x}})$). $\varepsilon_{ij}(\tilde{\mathbf{u}})$ are the strain components for the displacements $\tilde{\mathbf{u}}$ in point $\tilde{\mathbf{x}}$. Once again, the stationary condition relative to the optimisation variable is defined, in this case the microstructural density μ, as

$$\frac{\partial D^{\mathrm{h}}_{ijkl}(\mu)}{\partial \mu} \varepsilon_{ij}(\tilde{\mathbf{u}}) \varepsilon_{kl}(\tilde{\mathbf{u}}) - 2 \frac{\partial \beta^{\mathrm{h}}_{ij}(\mu)}{\partial \mu} \varepsilon_{ij}(\tilde{\mathbf{u}}) \Delta T = \lambda(\tilde{\mathbf{x}}) , \tag{67}$$
$$\forall \mathbf{y} \in Y(\tilde{\mathbf{x}}) , \text{ with } 0 < \mu < 1 ,$$

where

$$\frac{\partial D^{\mathrm{h}}_{ijkl}(\mu)}{\partial \mu} = \frac{1}{|Y|}\int_Y p\mu^{p-1} D^0_{pqrs}\left(\delta_{rk}\delta_{sl} - \frac{\partial \chi^{kl}_r}{\partial y_s}\right)\left(\delta_{pi}\delta_{qj} - \frac{\partial \chi^{ij}_p}{\partial y_q}\right)\mathrm{d}Y \tag{68}$$

and

$$\frac{\partial \beta^{\mathrm{h}}_{ij}(\mu)}{\partial \mu} = \frac{1}{|Y|}\int_Y \left(2p\mu^{2p-1} D^0_{ijkl}\alpha^0_{kl} - p\mu^{p-1} D^0_{ijkl}\frac{\partial \Psi_k}{\partial y_l}\right)\mathrm{d}Y \tag{69}$$

are the sensitivities of the homogenised tensors of elasticity, $\mathbf{D}^{\mathrm{h}}$, and thermal expansion moduli, $\boldsymbol{\beta}^{\mathrm{h}}$, respectively, to the variation of μ. As was the case for the global problem, these conditions become inequalities at the extremes. Condition 67 must be satisfied, for each $\mathbf{x}$ in Ω, at every $\mathbf{y}$ of the representative unit-cell.
The Lagangian 66 represents the local problem at the optimum, defined by the objective function $\Phi(\rho, \tilde{\mathbf{u}})$ (Eq. 61). From the definition of the Lagrange multiplier method, at the optimum $\tilde{\mathbf{x}}$,

$$\frac{\partial \Phi(\rho, \tilde{\mathbf{u}})}{\partial \rho} = \lambda(\tilde{\mathbf{x}})\,,\ \forall \tilde{\mathbf{x}} \in \Omega\,. \tag{70}$$

From this, according to equations 64 and 67, results

$$\frac{\partial D^{\mathrm{h}}_{ijkl}(\mu)}{\partial \mu}\varepsilon_{ij}(\tilde{\mathbf{u}})\varepsilon_{kl}(\tilde{\mathbf{u}}) - 2\frac{\partial \beta^{\mathrm{h}}_{ij}(\mu)}{\partial \mu}\varepsilon_{ij}(\tilde{\mathbf{u}})\Delta T = \lambda(\tilde{\mathbf{x}}) = 2\Lambda\,, \tag{71}$$
$$\forall \mathbf{y} \in Y(\tilde{\mathbf{x}})\,,\ \text{with}\ 0 < \mu < 1\,,$$

providing a conection between the optimal necessary conditions of both scales.

4.3 Hierarchical thermal problem

The presented hierarchical structure can be seamlessly adapted to the thermal problem. Note that both thermal and mechanical problems are formally identical. On one hand, both are defined by a typical conservation problem, with specific constitutive and compatibility relations and boundary conditions. On the other hand, both applications can have the objectives defined in terms of the maximisation of a constitutive constant, *i.e.* stiffness and conductivity. In this sense, as done for the objective definition of equation 62, the thermal compliance minimisation (or conductivity maximisation) can be defined for a thermal problem (see Eq. 13), ignoring convective and radiative terms ($Q = h_c = 0$), as

$$\min_{\substack{\rho(\mathbf{x}) \\ 0\le\rho(\mathbf{x})\le 1 \\ \int_\Omega \rho(\mathbf{x})\mathrm{d}\Omega \le V \\ \mathbf{K}_{\mathrm{T}}\mathbf{T}=\mathbf{q}}} \left[\frac{1}{2}\int_\Omega \Theta(\rho, \mathbf{T})\mathrm{d}\Omega\right]\,, \tag{72}$$

where

$$\Theta(\rho, \mathbf{T}) = \max_{\substack{\mu(\mathbf{x},\mathbf{y}) \\ 0\le\mu(\mathbf{x},\mathbf{y})\le 1 \\ \int_Y \mu(\mathbf{x},\mathbf{y})\mathrm{d}Y = \rho(\mathbf{x})}} k^{\mathrm{h}}_{ij}(\mu) T'_i T'_j\,, \quad \text{with} \quad T'_k = \frac{\partial T}{\partial y_k}\,. \tag{73}$$

Function Θ is equivalent to the strain energy density function of the thermoelastic problem for a thermal problem and is associated to the principle of virtual temperatures, which is in turn equivalent to the principle of virtual work (Bathe, 1996; Cook et al., 1989). It is a measure of thermal compliance, being used for the maximisation of the thermal conductivity for the macrostructural point $\mathbf{x}$ of Ω. T'_k and k^{h}_{ij} are the components of the temperature gradient and of the homogenised thermal conductivity tensor, respectively (see Eq. 30).
The definition of the optimisation problem and optimality conditions are equivalent to those of the previous section. It is however convenient to define the sensitivity of the homogenised thermal conductivity tensor to the variation of μ, given as

$$\frac{\partial k^{\mathrm{h}}_{ij}(\mu)}{\partial \mu} = \frac{1}{|\mathrm{Y}|}\int_{\mathrm{Y}} p\mu^{p-1}k^0_{rs}\left(\delta_{ri}-\frac{\partial \mathrm{Y}^i}{\partial y_r}\right)\left(\delta_{sj}-\frac{\partial \mathrm{Y}^j}{\partial y_s}\right)\mathrm{d}Y \tag{74}$$

Note that this problem can be solved independently or in a multiobjective approach. In this case, both thermal and mechanical objectives influence the objective function as (Challis et al., 2008; Chen et al., 2010; de Kruijf et al., 2007)

$$\min_{\substack{\rho(\mathbf{x})\\ 0\leq\rho(\mathbf{x})\leq 1\\ \int_\Omega \rho(\mathbf{x})\mathrm{d}\Omega\leq V\\ \mathbf{Ku}=\mathbf{f}\\ \mathbf{K}_{\mathrm{T}}\mathbf{T}=\mathbf{q}}} \quad w^{\mathrm{t}}\frac{F^{\mathrm{t}}}{F^{\mathrm{t}}_0}+w^{\mathrm{m}}\frac{F^{\mathrm{m}}}{F^{\mathrm{m}}_0}\,, \tag{75}$$

where F^{t} and F^{m} are the thermal and mechanical objective functions, respectively. F^{t}_0 and F^{m}_0 are normalisation terms, usually the respective objective values for the initial solution, and the values w^{t} and w^{m} are pondering weights for each objective. These weights can be used for the construction of Pareto fronts and are defined as $w^{\mathrm{m}} = 1 - w^{\mathrm{t}}$, with $w^{\mathrm{m}} \in [0,1]$ (Frischknecht et al., 2010).

5. Inverse homogenisation

The previous methodology, because of the clear separation of the problem in two distinct scales, provides a further utility. It is possible to sue the inner problem to perform local optimisation. Thus, ideal cellular or composite microstructures can be obtained as an optimal answer to a prescribed far-field. This is commonly called as local anysotropic problem or inverse homogenisation method.
The definition of this problem, equivalent to the local problems seen before within the hierarchical structure (see Eqs. 59 and 73), can be expressed as

$$\Phi(\mu,\overline{\varepsilon},\overline{\Delta T}) = \max_{\substack{\mu(\mathbf{y})\\ 0\leq\mu(\mathbf{y})\leq 1\\ \int_Y \mu(\mathbf{y})\mathrm{d}Y=V}} \left[D^{\mathrm{h}}_{ijkl}(\mu)\overline{\varepsilon}_{ij}\overline{\varepsilon}_{kl} - 2\beta^{\mathrm{h}}_{ij}(\mu)\overline{\varepsilon}_{ij}\overline{\Delta T}\right]\,, \tag{76}$$

or

$$\Theta(\mu,\overline{\mathbf{T}'}) = \max_{\substack{\mu(\mathbf{y})\\ 0\leq\mu(\mathbf{y})\leq 1\\ \int_Y \mu(\mathbf{y})\mathrm{d}Y=V}} \left[k^{\mathrm{h}}_{ij}(\mu)\overline{T'}_i\overline{T'}_j\right]\,, \tag{77}$$

as it concerns a thermomecanic or a thermal problem, respectivelly. $\bar{\varepsilon}$, $\overline{\Delta T}$ and $\overline{\mathbf{T}'}$ are strain, temperature difference and temperature gradient far-field prescribed values, respectively. The objectives of these problems are maximising the stiffness or thermal conductivity of the material. Once again, these problems can be solved within a multiobjective application.

6. Local approach

There are several approaches to solve material distribution problems for a given structural analysis application. In this work, as an alternative to the inverse homogenisation, a different strategy is also referred. Called by the authors optimisation local approach, it consists in the application of the typical single-scale topology optimisation problem to representative unit-cells, using specific periodic boundary conditions and asymptotic expansion homogenisation. The usual minimisation of the work of external loads or surface conduction heat fluxes (mechanical or thermal compliance) can be expressed as

$$\min_{\substack{0\leq\mu\leq 1 \\ \int_Y \mu(\mathbf{y})\mathrm{d}Y=\bar{\rho} \\ \mathbf{Ku}=\mathbf{f}}} \int_\Omega \Delta T\boldsymbol{\beta} : \boldsymbol{\varepsilon}(\mathbf{u})\mathrm{d}\Omega + \int_\Omega \mathbf{b}\cdot\mathbf{u}\mathrm{d}\Omega + \int_{\Gamma_{\mathrm{N_u}}} \bar{\mathbf{t}}\cdot\mathbf{u}\mathrm{d}\Gamma \tag{78}$$

or, using its practical implementation counterpart expressed in matrix notation (Sigmund, 2001), as

$$\min_{\substack{0\leq\mu\leq 1 \\ \int_Y \mu(\mathbf{y})\mathrm{d}Y=\bar{\rho} \\ \mathbf{Ku}=\mathbf{f}}} \int_\Omega \mathbf{u}^{\mathrm{T}}\mathbf{K}\mathbf{u}\,\mathrm{d}\Omega\,, \tag{79}$$

for the thermoelasticity problem, and

$$\min_{\substack{0\leq\mu\leq 1 \\ \int_Y \mu(\mathbf{y})\mathrm{d}Y=\bar{\rho} \\ \mathbf{K}_{\mathrm{T}}\mathbf{T}=\mathbf{q}}} \int_{\Gamma_{N_{\mathrm{T}}}} \bar{q}T\mathrm{d}\,\Gamma\,, \tag{80}$$

or, using its practical implementation counterpart expressed in matrix notation, as

$$\min_{\substack{0\leq\mu\leq 1 \\ \int_Y \mu(\mathbf{y})\mathrm{d}Y=\bar{\rho} \\ \mathbf{K}_{\mathrm{T}}\mathbf{T}=\mathbf{q}}} \int_\Omega \mathbf{T}^{\mathrm{T}}\mathbf{K}_{\mathrm{T}}\mathbf{T}\mathrm{d}\Omega \tag{81}$$

for the thermal problem (de Kruijf et al., 2007). The main difference to a typical macroscale topology optimisation problem resides on the use of boundary conditions. Using a far-field approach, the prescribed fields used in the inverse homogenisation are directly imposed in this case. Furthermore, not only strains and temperature gradients can be used in this case, but also stress and flux far-field states, applied as natural ou essential constraints. They are transformed in adequate boundary conditions to solve the finite element problems shown on the restrictions of the optimisation problem. These must enforce periodicity but in a broader sense than referred before. The periodicity boundary conditions used in the AEH restrict the overal deformation of the RUC, only allowing oscillations and maintaining an average

value equal to zero. In this case, the RUC is forced to deform according to the far-field values imposed, while still guaranteeing periodicity of the deformed state. In this case, not only two degrees of freedom are restricted in each boundary condition but three, using a control node to provide the adequate response of the RUC. After the convergence of the optimisation step, AEH is used to evaluate the constitutive properties of the obtained material.

7. Numerical details

The numerical approach to the presented procedures is dependent on several factors. In the context of this chapter, the authors make some general considerations over the finite element method (FEM) and clarify some aspects related to periodicity boundary conditions.
The general case of the optimisation problems shown here in the form of the hierarchical multiscale problem has a very high computational cost. Note that it requires two finite element models, each one discretising each scale. Moreover, the computational requirements are worsened from the fact that most of the time consumed in topology optimisation problem solving is spent on the finite element method equation solving (Bendsøe, 1995). The hierarchical structure needs, for each iteration, several FEM solutions. On one hand, the macroscale equilibrium problem. On the other hand, for each point on the macroscale (usually each finite element), an asymptotic expansion homogenisation problem is solved over the microscale discretisation. This, in itself, consists in several systems of equations to solve. Note that, for a two-dimensional problem, the elasticity problem requires three systems of equations, the thermal expansion one more and the thermal problem a further two. For the three-dimensional case, these values become six, one and three, respectively. Another aspect of these local problems, including the local approach, is related to conditioning problems, since the penalty method used here to enforce periodicity boundary conditions tends to unbalance the equations and to slow the convergence of the solver (Oliveira et al., 2010).
In what concerns the optimisation problem and variable update cycles, the authors use specific implementations of Optimality Criteria methods and Krister Svanberg's Method of Moving Asymptotes (MMA) (Bendsøe & Sigmund, 2003; Coelho et al., 2008; Svanberg, 1987).

7.1 Boundary conditions

At this point, it is important to clarify the use of periodicity boundary conditions, which are essential to the methodologies briefly shown in this chapter. Periodicity boundary conditions are imposed over the surface boundaries of the RUC (see Fig. 4) and shown here for a purely elastic case. Their usage for the thermal problem is almost seamless. The type of boundary condition used in this work is called Multi-Freedom Constraint (MFC), as opposed to the more usual Single-Freedom Constraint (SFC).
Starting with the periodicity boundary conditions used in the AEH, for a hexahedral unit-cell in $y_1 \in [0, y_1^0]$, $y_2 \in [0, y_2^0]$ and $y_3 \in [0, y_3^0]$ (see Fig. 4b), the boundary conditions can be defined, for the more general 3-D case, as

$$\begin{aligned} &\boldsymbol{\chi}(0, y_2, y_3) - \boldsymbol{\chi}(y_1^0, y_2, y_3) = \mathbf{0}\,, \\ &\boldsymbol{\chi}(y_1, 0, y_3) - \boldsymbol{\chi}(y_1, y_2^0, y_3) = \mathbf{0} \quad \text{and} \\ &\boldsymbol{\chi}(y_1, y_2, 0) - \boldsymbol{\chi}(y_1, y_2, y_3^0) = \mathbf{0}\,, \end{aligned} \tag{82}$$

where $\boldsymbol{\chi}$ is the corrector field for the elasticity homogenisation problem, which represents the mechanical characteristic displacement field tensor. In order to prevent rigid body motion,

displacements and rotations of an arbitrary point of the unit-cell must be locked or, since the MFCs are homogeneous (*i.e.* the independent value is equal to zero), the translation degrees of freedom of the vertices of the RUC must be restricted.

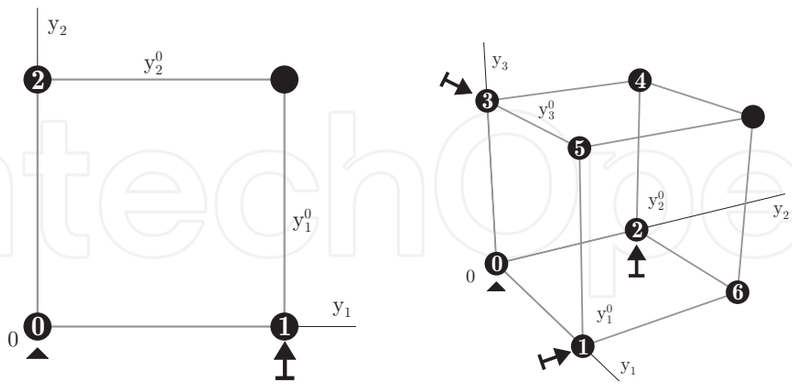

Fig. 4. Periodic RUC: (a) quadrilateral (2-D) and (b) hexahedral (3-D).

The second case in analysis is used on the local approach optimisation problem. This method allows the imposing of far-field stress or far-field strain. The imposing of a macroscale stress-state $\boldsymbol{\sigma}$ over the RUC (*e.g.* taken from a integration point of the main structure finite element mesh) may be done calculating the equivalent loads ($\mathbf{P}$) over the RUC. This is done over the boundaries (Γ) of the unit-cell, where (Böhm, 1998)

$$\mathbf{P} = \int_{\Gamma} \bar{\mathbf{t}}_{\mathrm{a}}(\mathbf{y}) \mathrm{d}\Gamma, \quad \text{with} \quad \bar{\mathbf{t}}_{\mathrm{a}} = \boldsymbol{\sigma}_{\mathrm{a}} \cdot \mathbf{n}\,. \tag{83}$$

Here, $\bar{\mathbf{t}}_{\mathrm{a}}$ stands for the homogeneous surface traction vector corresponding to the applied (far-field) stress $\boldsymbol{\sigma}_{\mathrm{a}}$ at a given point on the cell's surface and $\mathbf{n}$ is the local surface outward unit vector. The numerical imposing of the equivalent loads involves multiplying a given stress component by the surface area of the boundary at a given element and distributing it to the connected boundary nodes. This equivalent load field must be antiperiodic for equilibrium to be fulfiled. On the other hand, in order to guarantee periodicity there must also be adequate MFCs. These are homogeneous, but, where the homogenisation application renders only oscillations around an average state, these must allow for the global deformation of the RUC. Thus, the vertices cease to be fixed and each MFC connects more than two nodes. The single-freedom constraints (SFCs) used are illustrated in figure 4, preventing rigid body motion by restricting 3 DOFs for the 2-D case and 6 DOF for the 3-D case. The MFCs use control vertices to pull the other nodes and guarantee periodicity. The resulting MFCs may be presented as

$$\begin{aligned} \mathbf{u}(y_1^0, y_2) &= \mathbf{u}(0, y_2) + \mathbf{u}_1 \quad \text{and} \\ \mathbf{u}(y_1, y_2^0) &= \mathbf{u}(y_1, 0) + \mathbf{u}_2\,, \end{aligned} \tag{84}$$

for the 2-D case, and

$$\begin{aligned} \mathbf{u}(y_1^0, y_2, y_3) &= \mathbf{u}(0, y_2, y_3) + \mathbf{u}_1\,, \\ \mathbf{u}(y_1, y_2^0, y_3) &= \mathbf{u}(y_1, 0, y_3) + \mathbf{u}_2 \quad \text{and} \\ \mathbf{u}(y_1, y_2, y_3^0) &= \mathbf{u}(y_1, y_2, 0) + \mathbf{u}_3\,, \end{aligned} \tag{85}$$

for the 3-D case.
For the last case, the macroscale strains $\boldsymbol{\varepsilon}$ are, as for the stress, imposed as a far-field state. The main difference to the previous case is that the RUC isn't deformed using Neumann boundary conditions, but only Dirichlet boundary conditions. The localisation is done forcing equivalent displacements that render an average strain equal to the macroscale strain. This is done, for the 2-D and 3-D cases, using the non-homogeneous conditions

$$\begin{aligned} \mathbf{u}(y_1^0, y_2) - \mathbf{u}(0, y_2) &= \mathbf{c}_1 \quad \text{and} \\ \mathbf{u}(y_1, y_2^0) - \mathbf{u}(y_1, 0) &= \mathbf{c}_2 \,, \end{aligned} \tag{86}$$

and

$$\begin{aligned} \mathbf{u}(y_1^0, y_2, y_3) - \mathbf{u}(0, y_2, y_3) &= \mathbf{c}_1 \,, \\ \mathbf{u}(y_1, y_2^0, y_3) - \mathbf{u}(y_1, 0, y_3) &= \mathbf{c}_2 \quad \text{and} \\ \mathbf{u}(y_1, y_2, y_3^0) - \mathbf{u}(y_1, y_2, 0) &= \mathbf{c}_3 \,, \end{aligned} \tag{87}$$

respectively. In this case, instead of the homogeneous three-node conditions used in equations 84 and 85, two-node non-homogeneous conditions are used, using the independent coefficients $\mathbf{c}$. These constants are calculated to match the imposed strain states. Yet another alternative configuration can be obtained with the same MFCs used in the stress-based case. Using the same homogeneous conditions to enforce periodicity, the Dirichlet condition can be imposed on the control vertices, rendering the same effect, *i.e.* adding the conditions

$$\begin{aligned} \mathbf{u}_1 - \mathbf{u}_0 &= \mathbf{c}_1 \,, \\ \mathbf{u}_2 - \mathbf{u}_0 &= \mathbf{c}_2 \quad \text{and} \\ \mathbf{u}_3 - \mathbf{u}_0 &= \mathbf{c}_3 \end{aligned} \tag{88}$$

to the homogeneous MFCs used before. Note that the third condition is used only for the 3-D case. Additionally, note that $\mathbf{u}_0 = \mathbf{0}$, which makes equations 88 correspond to single-freedom essential boundary conditions.

8. Examples

In the scope of this chapter, the authors show some representative examples of applications of the methods summed within the previous sections. In this sense, the Asymptotic Expansion Homogenisation is the main topic. As such, results of the associated AEH procedures are shown explicit or implicitly for most examples. Different applications and levels of multiscale optimisation are also shown. All of these examples were solved in a totally in-house developed code. This code, developed by the authors, uses the finite element method to solve 2-D and 3-D problems, with several different linear and quadratic elements, and a conjugate gradient iterative parallel solver. It solves problems in linear thermoelasticity with homogenisation and automatic degree of freedom association and periodicity boundary condition enforcing. Moreover, it is able to solve topology optimisation multiscale problems, using variations of power-law methods, optimality criteria and MMA (Svanberg, 1987).
The first example (Oliveira et al., 2009) shows a typical AEH application. In this linear elastic case, a given structure is subjected to a tensile stress. The material used to build this structure is represented using the discretisation shown in figure 5(a) and models an $AlSiC_p$ MMC with 30% volume fraction of SiC particles. The macroscale uses a structured hexahedra mesh and

the microscale an non-structured non-periodic tetrahedra mesh. Figures 5(b) to (g) show the 6 eigenshapes χ_{kl} associated to the characteristic displacements of the representative unit-cell, from which the oscillations that solve the local problem and allow the evaluation of the constitutive properties are processed. Furthermore, these oscillations are also used in the localisation procedure. In figure 6 it is possible to see the microscale stress field for a given element and Gauss point. As expected, the macroscale stress value sits within the microscale limits, as the material heterogeneities impose detailed stress oscillations (Oliveira et al., 2009).

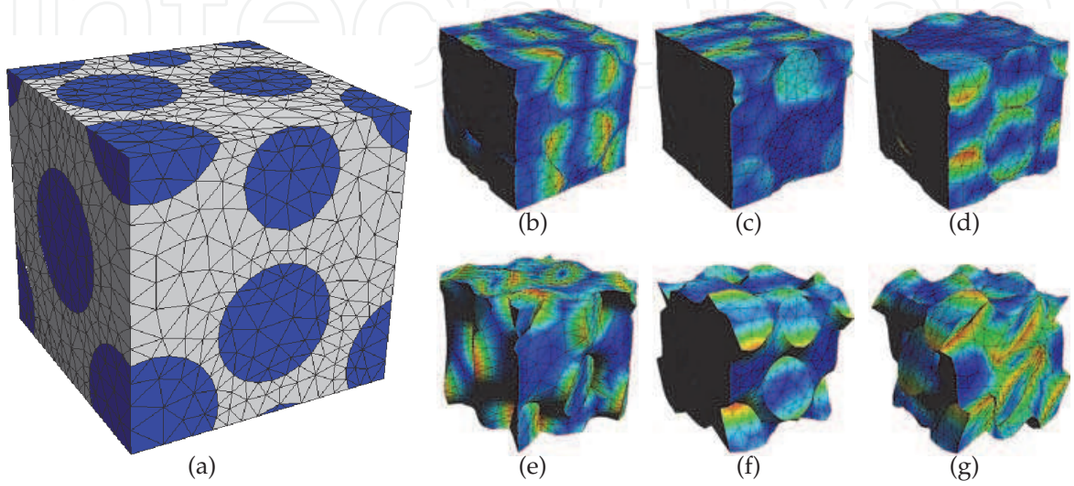

Fig. 5. Unstructured and non-periodic RUC finite element mesh (microscale). Characteristic displacements for the 30% reinforcement RUC: normal eigenshapes (a) χ_{11}, (b) χ_{22}, (c) χ_{33} and shear eigenshapes (d) χ_{12}, (e) χ_{23}, (f) χ_{13} (Oliveira et al., 2009).

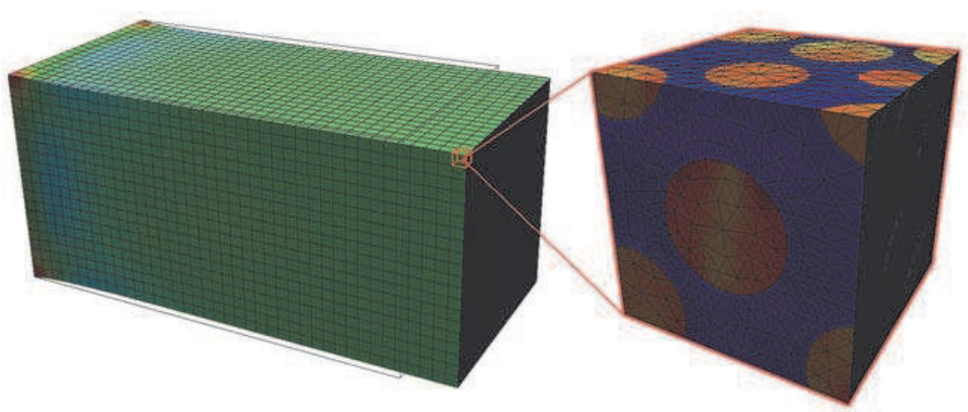

Fig. 6. Equivalent von Mises stress on the microscale, obtained with the localisation procedure on a Gauss point of a macroscale finite element (Oliveira et al., 2009).

As a second example, figure 7 shows the use of single-scale structural topology optimisation using different constitutive properties. In this case, a RUC of aluminium (Al) matrix reinforced with boron (B) continuous parallel fibres, with a reinforcement volume fraction of 47%, was used. Applying the asymptotic expansion homogenisation procedure led to an elasticity matrix for this three-dimensional composite material structure. Three different

bidimensional elasticity matrices were derived, each representing the material properties of the composite material for each of the three main orthogonal orientations. This resulted in the two orthogonal orthotropic and one cubic orientations illustrated in figure 7. These material properties were then used in the macroscale topology optimisation problem with the shown set of boundary conditions. It is clear that, for a constant reinforcement volume fraction, the microscale topology has a major influence on the optimal macrostructure design. Furthermore, the two orthotropic examples act as bounds for the isotropic case. It is also possible to verify the influence of the reinforcement orientation on the optimisation results.

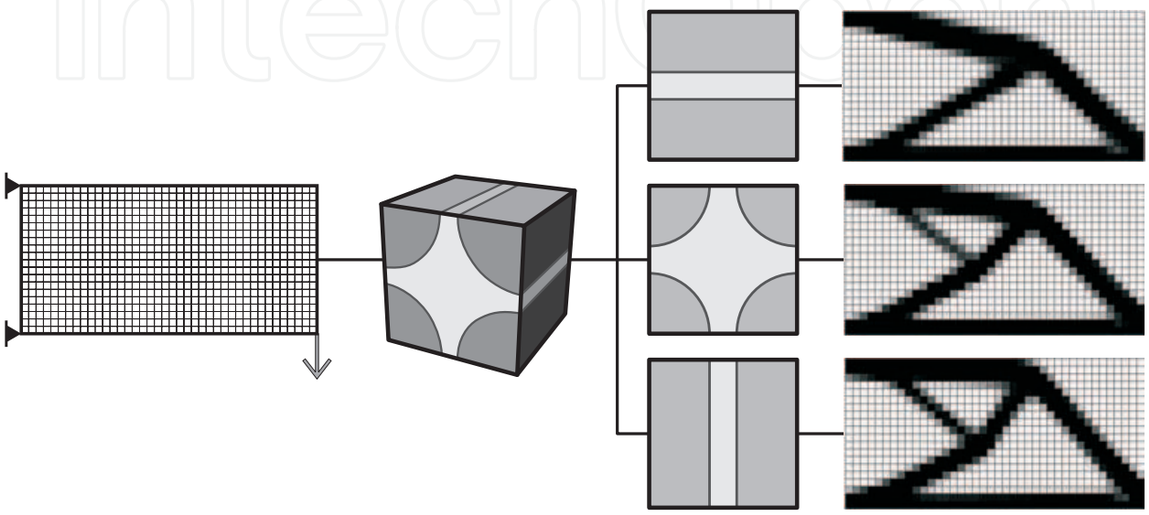

Fig. 7. Topology optimisation results using different reinforcement orientations.

A further application shows the multiobjective optimisation of simultaneously a mechanical and thermal problem. In this case, the local approach is applied to the compliance minimisation problem. The minimisation of these functions frequently results in conflicting objectives, as the resulting structures range from maximum stiffness to maximum heat dissipation (maximum conductivity). Figure 8 shows the Pareto front that arises from the maximisation of the stiffness of a 2-D RUC ($f_{\mathrm{v}} = 0.5$) over the vertical direction and the simultaneous maximisation of the thermal conductivity over a horizontal direction. The presented values are normalised, using each initial compliance. It is noteworthy that utopia solutions are different from Pareto optimal solutions, since objectives are conflicting. Figure 9 shows the characteristic fields (linear thermal expansion – $\mathbf{\Psi}$, thermal conductivity – $\mathbf{\Upsilon}$, and stiffness – $\boldsymbol{\chi}$), for a thermal problem weight of $w^{\mathrm{t}} = 0.4$. The same is shown for a 3-D RUC example, with $w^{\mathrm{t}} = 0.5$ and subjected to far-field stress ($\boldsymbol{\sigma} = \{1; 0; -1; 0; 0; 0\}$) and heat flux ($\mathbf{q} = \{0.5; 0.25; 1\}$) states.

An alternative to the local approach shown before is the use of the inverse optimisation. Figure 11 shows the optimal microstructure obtained when using this methodology for a mechanical problem, with a macroscopic strain of $\boldsymbol{\varepsilon} = \{0; 0; 0; 1; 1; 1\}$. Is is possible to see both the stiff and soft material phases. The composite material constituents have Young's moduli related as $d_{\mathrm{m}} = E_1/E_2 = 100$. A periodicity illustration is shown for this material distribution, showing that the method complies perfectly with this requirement. Furthermore, an anisotropy spherical plot shows the stiffness of this material along each direction, evaluated through the application of the AEH procedure. Once more, the characteristic displacements that result from the material distribution and the AEH methodology are also illustrated.

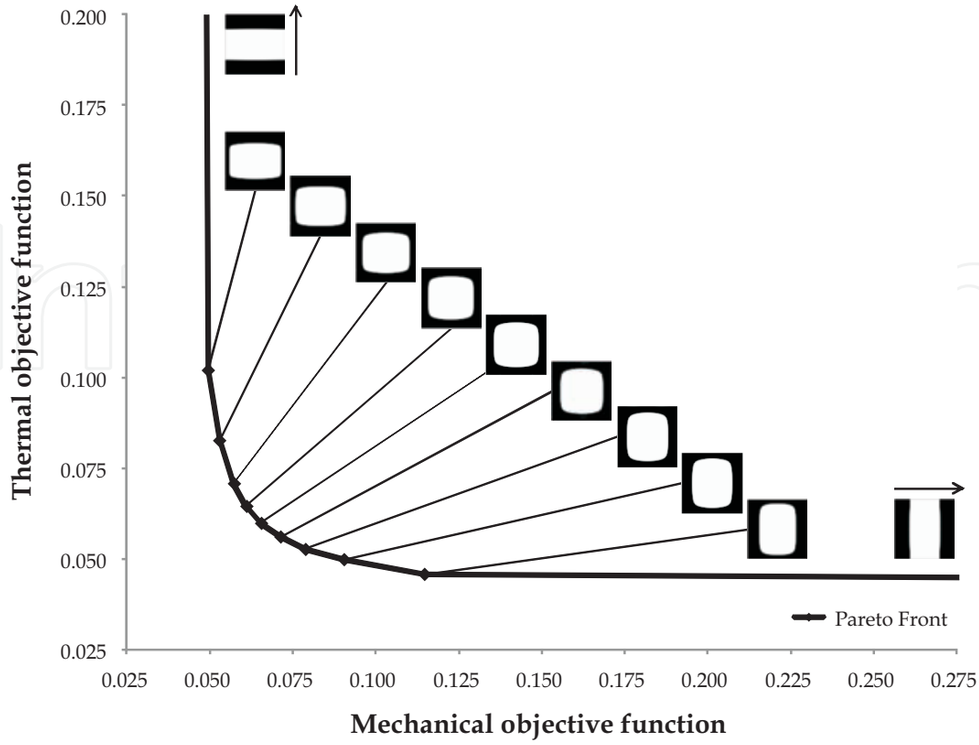

Fig. 8. Square RUC microscale optimisation results: Pareto front for a 2-D mechanical/thermal multiobjective problem.

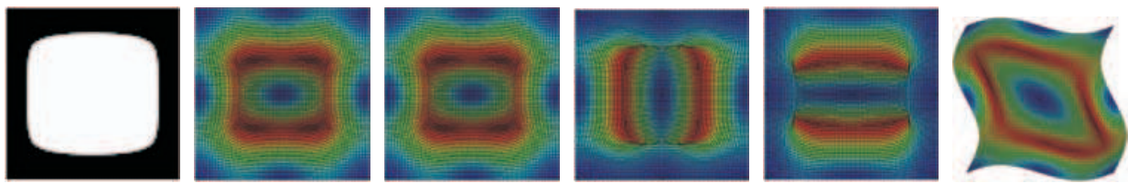

Fig. 9. Multiobjective topology optimisation, using the local approcah, for a 2-D RUC (w^t=0.4): (a) material distribution, (b) thermal expansion ($\mathbf{\Psi}$), (c) conductivity ($\mathbf{\Upsilon}$) and (d-e) χ_{11}, χ_{22} and χ_{12} characteristic displacement modes.

The previous example, in a hierarchical structure, can be used in applications as the following. In this case, for each iteration, a multiscale problem is solved. The global problem is solved on the macroscale, using constitutive information taken from the microscale. This problem leads to a strain field that can be used in different forms to control the microscale problem. In this first case, the strain field is averaged and pondered using the equivalent strain over the macroscale in a simplified hierarchical structure. All the macroscale is made of the same material, which constituent distribution in updated with the evolution of both the optimisation procedure and the macroscopic strain field. Figure 12 shows both the macroscale homogenenised problem and the optimal microscale solution that arises as a response to the global strains. The problem is a simultaneous bending and torsion test. The results show the results for both loads applied together (see Fig. 12(a)) or as part of a multiload case (see Fig. 12(b)).

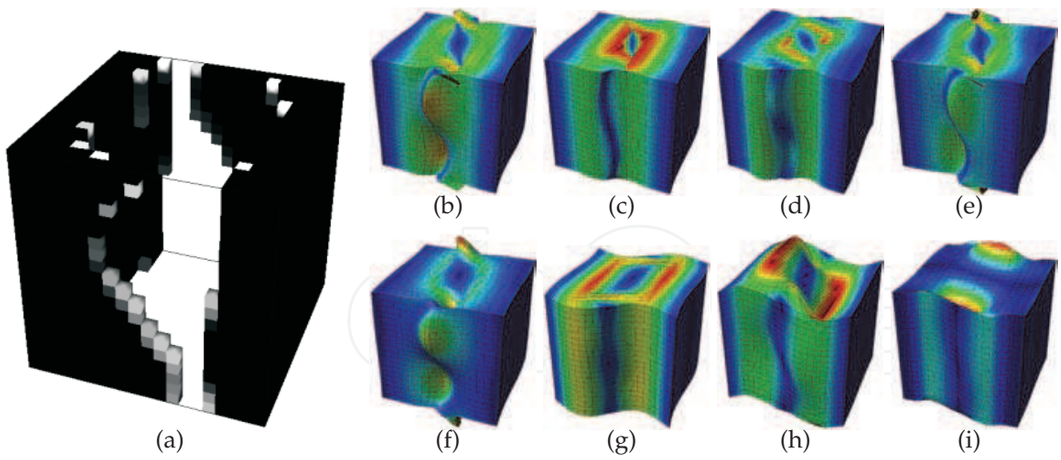

Fig. 10. Multiobjective topology optimisation, using the local approcah, for a 3-D RUC (w^{t}=0.5): (a) material distribution, (b) thermal expansion ($\mathbf{\Psi}$), (c) conductivity ($\mathbf{\Upsilon}$) and (d-i) $\boldsymbol{\chi}_{11}$, $\boldsymbol{\chi}_{22}$, $\boldsymbol{\chi}_{33}$, $\boldsymbol{\chi}_{12}$, $\boldsymbol{\chi}_{23}$ and $\boldsymbol{\chi}_{13}$ characteristic displacement modes.

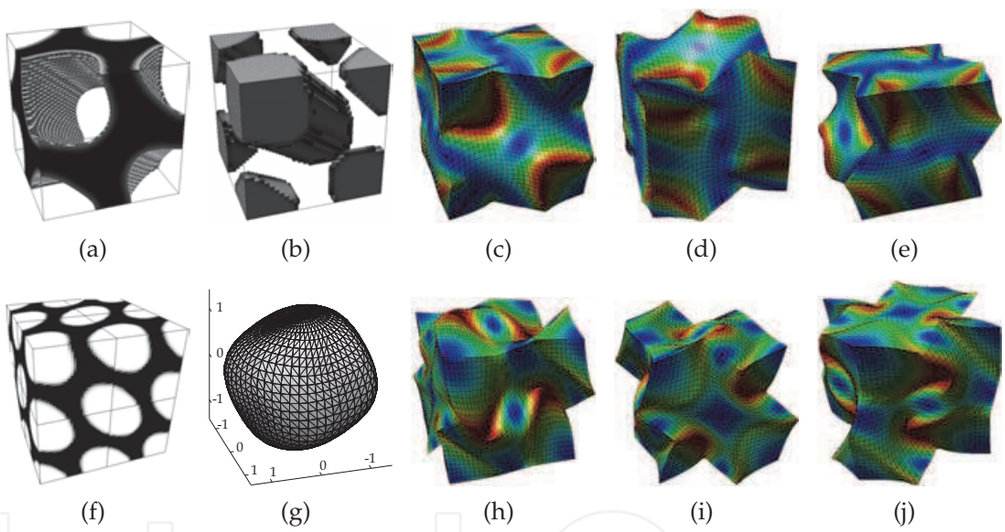

Fig. 11. Microscale topology optimisation, using the inverse homogenisation, for a 3-D RUC (ε=$\{0;0;0;1;1;1\}$): (a) stiff and (b) soft material distributions, (f) periodicity illustration, (g) anisotropy plot, and (c-e,h-j) $\boldsymbol{\chi}_{11}$, $\boldsymbol{\chi}_{22}$, $\boldsymbol{\chi}_{33}$, $\boldsymbol{\chi}_{12}$, $\boldsymbol{\chi}_{23}$ and $\boldsymbol{\chi}_{13}$ characteristic displacement modes.

The general case of the previous examples is the application of the hierarchical procedure, with concurrent optimisation of the material distribution over the two scales. Figure 13 shows such an application. The presented 2-D example uses a typical bycicle wheel mechanical optimisation problem and adds a thermal problem, for a multiobjective strategy. Both the mechanical and thermal boundary conditions are represented and the weight of the thermal problem is $w^{\mathrm{t}} = 0.75$. Some of the local problem solutions are also presented, giving the notion of effective material distribution, as well of the shear dimension of the problem, even for a 2-D case. This multiobjective procedure needs normalisation of the objectives, acting on the objective function and the sensitivities. Note that, even for this relaxed and filtered

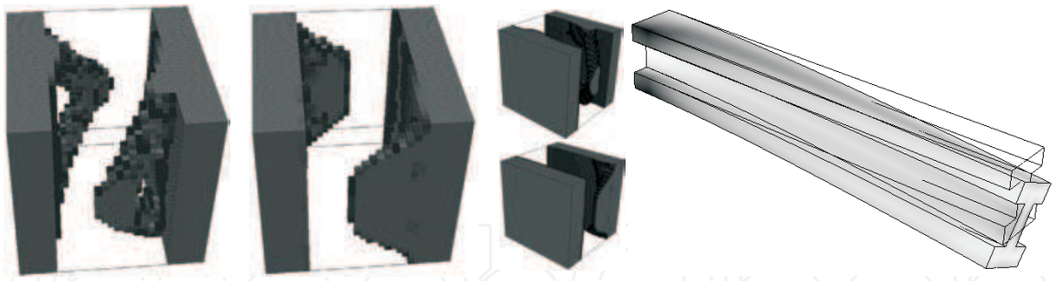

(a) (b) (c)

Fig. 12. Hierarchical problem with local topology optimisation: microscale optimal topology (stiff phase) for (a) bending and torsion and (b) bending and torsion as multiload cases, and (c) results with macroscale deformed state and stress isovalues.

solution, the macroscale density distribution still shows some checkerboard tendencies. This can be solved using higher-order finite elements but leads to an even higher computational cost.

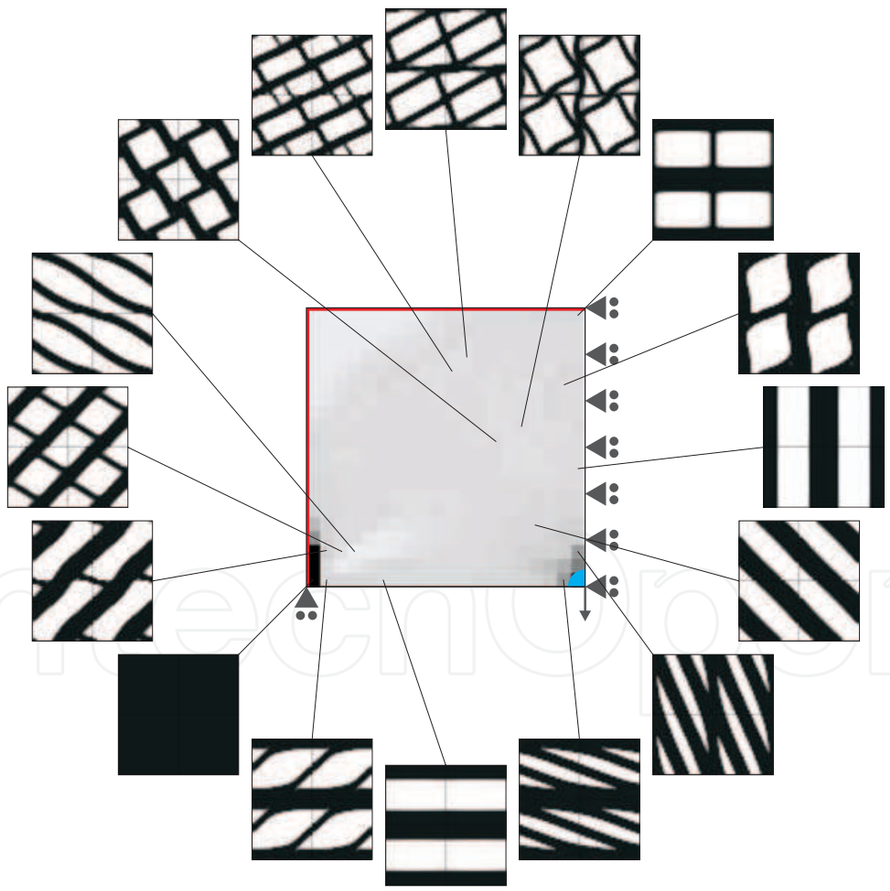

Fig. 13. Hierarchical multiobjective (thermal and mechanical) 2-D example (w^t=0.75), showing the macroscale density distribution and some local material distributions.

9. Final remarks

The main objective of this chapter was to give an overview of the Asymptotic Expansion Homogenisation, and its use both on the evaluation of effective properties of periodic structure composite and cellular materials and on the search for the optimal material for a given application. The procedures associated to these objectives are shown, for linear thermal an thermomechanical problems. Special emphasis is put on problem formulation and certain specific numerical details. Moreover, its usage in topology optimisation problems is shown to be varied, ranging from local optimisation to the full fledged hierarchical optimisation.
Nevertheless, in spite of the potential of these strategies, there are some shortcomings. First of all, the boundary conditions associated to these problems can become numerically problematic. On one hand, its implementation is not always straightforward. On the other hand, depending on the method used, they can lead to conditioning problems of the numerical equation systems and subsequent convergence problems and computational time increase. This is even more critical when considering optimisation problems. The varying local density distribution and the sometimes very high difference between numerical values within the systems of equations slows the problem solving down. If one adds this to the overall dimension of hierarchical multiscale problems, the problems rapidly approach limits that make them impossible to solve in conventional hardware.

10. Acknowledgements

The authors thank the financial support given by the Portuguese Foundation for Science and Technology (FCT – Fundação para a Ciência e a Tecnologia) and by the European Social Fund (FSE – Fundo Social Europeu) within the 3rd Community Support Framework.

11. References

Allaire, G. (2001). *Shape Optimization by the Homogenization Method*, 1st edn, Springer, New York, USA.

Arora, J. (2004). *Introduction to Optimum Design*, 2nd edn, Academic Press, San Diego, USA.

Bathe, K.-J. (1996). *Finite Element Procedures*, Prentice-Hall International Editions, Inc., New Jersey, USA.

Bendsøe, M.P. & Kikuchi, N. (1988). Generating optimal topologies in structural design using a homogenization method, *Computer Methods in Applied Mechanics and Engineering* 71(2): 197–224.

Bendsøe, M.P. (1995). *Optimization of Structural Topology, Shape, and Material*, Springer, Berlin, Germany.

Bendsøe, M.P. & Sigmund, O. (1999). Material interpolation schemes in topology optimization, *Archive of Applied Mechanics* 69(9-10): 635–654.

Bendsøe, M.P. & Sigmund, O. (2003). *Topology Optimization: Theory, Methods, and Applications*, Springer, Berlin, Germany.

Böhm, H.J. (1998). *A short introduction to basic aspects of continuum micromechanics*, CDL-FMD-Report, Christian Doppler Laboratorium für Mikromechanik der Werkstoffe, Institut für Leichtbau und Flugzeugbau, Technische Universität Wien, Vienna, Austria.

Challis, V.J., Roberts, A.P. & Wilkins, A.H. (2008). Design of three dimensional isotropic microstructures for maximized stiffness and conductivity, *International Journal of Solids and Structures* 45(14-15): 4130–4146.

Chen, Y., Zhou, S. & Li, Q. (2009). Multiobjective topology optimization for finite periodic structures, *Computers & Structures* 88(11-12): 806–811.

Cioranescu, D. & Donato, P. (1999). *An Introduction to Homogenization*, Oxford Lecture Series in Mathematics and Its Applications, Vol. 17, Oxford University Press, Oxford, United Kingdom.

Coelho, P.G., Fernandes, P.R., Guedes, J.M. & Rodrigues, H.C. (2008). A hierarchical model for concurrent material and topology optimisation of three-dimensional structures, *Structural and Multidisciplinary Optimization* 35(2): 107–115.

Cook, R.D., Malkus, D.S. & Plesha, M.E. (1989). *Concepts and Applications of Finite Element Analysis*, 3rd edn, John Wiley & Sons, New York, USA.

de Kruijf, N., Zhou, S., Li, Q. & Mai, Y.W. (2007). Topological design of structures and composite materials with multiobjectives, *International Journal of Solids and Structures* 44(22-23): 7092–7109.

Díaz, A. & Lipton, R. (1997). Optimal material layout for 3D elastic structures, *Structural and Multidisciplinary Optimization* 13(1): 60–64.

Frischknecht, B.D., Peters, D.L. & Papalambros, P.Y. (2010). Pareto set analysis: local measures of objective coupling in multiobjective design optimization, *Structural and Multidisciplinary Optimization* pp. 1–14. DOI: 10.1007/s00158-010-0599-2.

Fung, Y.C. & Tong, P. (2005). *Classical and Computational Solid Mechanics*, Advanced Series in Engineering Science, Vol. 1, World Scientific Publishing, Singapore.

Guedes, J.M. & Kikuchi, N. (1990). Preprocessing and postprocessing for materials based on the homogenization method with adaptive finite element methods, *Computer Methods in Applied Mechanics and Engineering* 83(2): 143–198.

Guedes, J.M., Lubrano, E. , Rodrigues, H.C. & Turteltaub, S. (2006). Hierarchical optimization of material and structure for thermal transient problems, *Proceedings of IUTAM Symposium on Topological Design Optimization of Structures, Machines and Materials: Status and Perspectives*, Springer, Bendsøe, M.P., Olhoff, N., Sigmund, O. (Eds.), Vol. 137, Rungstedgaard, Denmark, pp. 525-536.

Hassani, B. & Hinton, E. (1999). *Homogenization and Structural Topology Optimization: Theory, Practice, and Software*, Springer, London, United Kingdom.

Lewis, R.W., Morgan, K., Thomas, H.R. & Seetharamu, K.N. (1996). *The Finite Element Method in Heat Transfer Analysis*, John Wiley & Sons, Chichester, United Kingdom.

Oliveira, J.A., Pinho-da-Cruz, J. & Teixeira-Dias, F. (2009). Asymptotic homogenisation in linear elasticity. Part II: Finite element procedures and multiscale applications, *Computational Materials Science* 45(4): 1081–1096.

Oliveira, J.A., Pinho-da.Cruz, J., Andrade-Campos, A. & Teixeira-Dias, F. (2010). Stress- and strain-based multifreedom constraints for periodic media optimisation, *Proceedings of EngOpt2010 – 2nd International Conference on Engineering Optimisation*, APMTAC, Lisbon, Portugal, p. 148.

Pinho-da-Cruz, J. (2007). *Thermomechanical Characterisation of Multiphasic Materials Using Homogenisation Procedures*, PhD thesis (in portuguese), Universidade de Aveiro, Aveiro, Portugal.

Pinho-da-Cruz, J., Oliveira, J.A. & Teixeira-Dias, F. (2008). Homogenisation of composite materials in thermoelasticity: Formal mathematics and computational issues, *Proceedings of International Conference on Mathematics and Continuum Mechanics*, CIM, A.J.M. Ferreira, I.M.N. Figueiredo, J. Videman (Eds.), Vol. 30, Porto, Portugal, pp. 35-40.

Pinho-da-Cruz, J., Oliveira, J.A. & Teixeira-Dias, F. (2009). Asymptotic homogenisation in linear elasticity. Part I: Mathematical formulation and finite element modelling, *Computational Materials Science* 45(4): 1073–1080.

Rodrigues, H., Guedes, J. & Bendsøe, M.P. (2002). Hierarchical optimization of material and structure, *Structural and Multidisciplinary Optimization* 24(1): 1–10.

Sanchez-Hubert, J. & Sanchez-Palencia, E. (1992). *Introduction aux Méthodes Asymptotiques et à l'Homogénéisation: Application à la Mécanique des Milieux Continus*, Collection Mathématiques Appliquées pour la Maîtrise, Masson, Paris, France.

Sigmund, O. (2001). A 99 line topology optimization code written in Matlab, *Structural and Multidisciplinary Optimization* 21(2): 120–127.

Sigmund, O. (2007). Morphology-based black and white filters for topology optimization, *Structural and Multidisciplinary Optimization* 33(4-5): 401–424.

Svanberg, K. (1987). The method of moving asymptotes – a new method for structural optimization, *International Journal for Numerical Methods in Engineering* 24(2): 359–373.

Terada, K. (1996). *Global-Local Modeling for Composites by the Homogenization Method*, PhD thesis, University of Michigan, Ann Arbor, USA.

Theocaris, P.S & Stavroulakis, G.E. (1998). Multilevel optimal design of composite structures including materials with negative Poisson's ratio, *Structural and Multidisciplinary Optimization* 15(1): 8–15.

Theocaris, P. & Stavroulakis, G. (1999). Optimal material design in composites: An iterative approach based on homogenized cells, *Computer Methods in Applied Mechanics and Engineering* 169(1-2): 31–42.

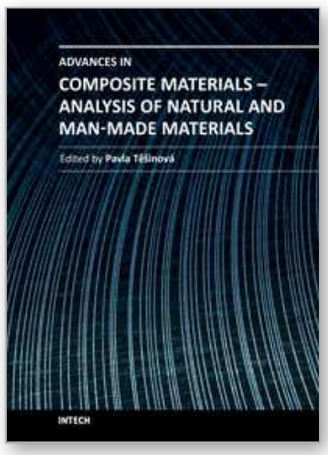

Advances in Composite Materials - Analysis of Natural and Man-Made Materials

Edited by Dr. Pavla Tesinova

ISBN 978-953-307-449-8
Hard cover, 572 pages
Publisher InTech
Published online 09, September, 2011
Published in print edition September, 2011

Composites are made up of constituent materials with high engineering potential. This potential is wide as wide is the variation of materials and structure constructions when new updates are invented every day. Technological advances in composite field are included in the equipment surrounding us daily; our lives are becoming safer, hand in hand with economical and ecological advantages. This book collects original studies concerning composite materials, their properties and testing from various points of view. Chapters are divided into groups according to their main aim. Material properties are described in innovative way either for standard components as glass, epoxy, carbon, etc. or biomaterials and natural sources materials as ramie, bone, wood, etc. Manufacturing processes are represented by moulding methods; lamination process includes monitoring during process. Innovative testing procedures are described in electrochemistry, pulse velocity, fracture toughness in macro-micro mechanical behaviour and more.

How to reference

In order to correctly reference this scholarly work, feel free to copy and paste the following:

João A. Oliveira, Joaquim Pinho-da-Cruz and Filipe Teixeira-Dias (2011). Asymptotic Expansion Homogenisation and Multiscale Topology Optimisation of Composite Structures, Advances in Composite Materials - Analysis of Natural and Man-Made Materials, Dr. Pavla Tesinova (Ed.), ISBN: 978-953-307-449-8, InTech, Available from: http://www.intechopen.com/books/advances-in-composite-materials-analysis-of-natural-and-man-made-materials/asymptotic-expansion-homogenisation-and-multiscale-topology-optimisation-of-composite-structures

INTECH
open science | open minds

InTech Europe
University Campus STeP Ri
Slavka Krautzeka 83/A
51000 Rijeka, Croatia
Phone: +385 (51) 770 447
Fax: +385 (51) 686 166
www.intechopen.com

InTech China
Unit 405, Office Block, Hotel Equatorial Shanghai
No.65, Yan An Road (West), Shanghai, 200040, China
中国上海市延安西路65号上海国际贵都大饭店办公楼405单元
Phone: +86-21-62489820
Fax: +86-21-62489821

IntechOpen